Appl Microbiol Biotechnol (2011) 92:617–630
DOI 10.1007/s00253-011-3556-0

METHODS AND PROTOCOLS

Microbial synthesis of gold nanoparticles using the fungus *Penicillium brevicompactum* and their cytotoxic effects against mouse mayo blast cancer C_2C_{12} cells

Amrita Mishra · Suraj Kumar Tripathy · Rizwan Wahab · Song-Hoon Jeong · Inho Hwang · You-Bing Yang · Young-Soon Kim · Hyung-Shik Shin · Soon-Il Yun

Received: 16 May 2011 / Revised: 9 August 2011 / Accepted: 17 August 2011 / Published online: 6 September 2011
© Springer-Verlag 2011

Abstract Microorganisms, their cell filtrates, and live biomass have been utilized for synthesizing various gold nanoparticles. The shape, size, stability as well as the purity of the bio synthesized nanoparticles become very essential for application purpose. In the present study, gold nanoparticles have been synthesized from the supernatant, live cell filtrate, and biomass of the fungus *Penicillium brevicompactum*. The fungus has been grown in potato dextrose broth which is also found to synthesize gold nanoparticles. The size of the particles has been investigated by Bio-TEM before purification, following purification and after storing the particles for 3 months under refrigerated condition. Different characterization techniques like X-ray diffraction, Fourier transform infrared spectroscopy, and UV–visible spectroscopy have been used for analysis of the particles. The effect of reaction parameters such as pH and concentration of gold salt have also been monitored to optimize the morphology and dispersity of the synthesized gold nanoparticles. A pH range of 5 to 8 has favored the synthesis process whereas increasing concentration of gold salt (beyond 2 mM) has resulted in the formation of bigger sized and aggregated nanoparticles. Additionally, the cytotoxic nature of prepared nanoparticles has been analyzed using mouse mayo blast cancer C_2C_{12} cells at different time intervals (24, 48, and 72 h) of incubation period. The cells are cultivated in Dulbecco's modified Eagle's medium supplemented with fetal bovine serum with antibiotics (streptopenicillin) at 37°C in a 5% humidified environment of CO_2. The medium has been replenished every other day, and the cells are subcultured after reaching the confluence. The viability of the cells is analyzed with 3-(4, 5-dimethylthiazol-2-yl)-2, 5-diphenyltetrazolium bromide method.

Keywords *Penicillium brevicompactum* · Gold nanoparticles · Live cell filtrate · pH value · Gold ion concentration · Cytotoxicity

A. Mishra · S.-H. Jeong · S.-I. Yun (✉)
Department of Food Science & Technology, College of Agriculture & Life Sciences, Chonbuk National University, Jeonju 561-756, Republic of Korea
e-mail: siyun@jbnu.ac.kr

S. K. Tripathy
Korea Institute of Machinery & Materials, Daejeon 305-343, Republic of Korea

R. Wahab · Y.-S. Kim · H.-S. Shin
Department of Chemical Engineering, College of Engineering, Chonbuk National University, Jeonju 561-756, Republic of Korea

R. Wahab · I. Hwang · Y.-B. Yang
Department of Animal Resources & Biotechnology, College of Agriculture & Life Sciences, Chonbuk National University, Jeonju 561-756, Republic of Korea

Introduction

The therapeutic activity of cytotoxic agents is often limited owing to their selectivity in targeting cancer cells. New systemic therapies have to be developed that can overcome nonspecific uptake by mononuclear phagocytic cells and by other nontargeted cells. Particles synthesized in the nano-range are acting as potential carriers as an alternative to existing cancer therapies (Ferrari 2005; Peer et al. 2007). Many different systems have attracted interest among researchers, originally starting with polymeric drugs, continuing later with stealth liposomes, while the focus today is shifting toward polymeric and inorganic nanoparticles (Peer et al. 2007; Torchilin 2006). Several nanoparticles including gold nanoparticles have already been

used for therapeutic and diagnostic applications (Huang et al. 2007). The shift in focus to nanotechnology in the recent past is also attributed to several other reasons. Particles synthesized in the nanorange are significantly different from those of bulk materials. The size-dependent properties displayed by such particles make them superior and indispensable in several areas (William 2004; Kulkarni 2007). Owing to their wide range of applications in several fields, gold and silver nanoparticles have already been synthesized using different microorganisms as well as plant extracts in an effort to develop an alternative green technology route to chemically synthesized nanoparticles (Park et al. 2010; Shankar et al. 2003; Mandal et al. 2006; Gardea-Torresdey et al. 2002; Mukherjee et al. 2002; Ahmad et al. 2003a, b; Mishra et al. 2011; Chandran et al. 2008). Using plant extracts over microorganisms for biosynthesis has certain disadvantages as complete aseptic environment is required for getting optimal result whereas under real condition maintaining such environment is not cost-effective. Over the years, several researchers are trying to focus on extracellular synthesis of nanoparticles as the method employed makes downstream processing less laborious and is cost-effective which is very important for industrial applications. Extracellular synthesis of nanoparticles is simpler with fungi as compared to bacteria and yeast since they generate more biomass which enables easy handling during biosynthesis. However, when nanoparticles are synthesized by microorganisms, optimizing the size and shape of synthesized particles is very necessary and essential for their effective industrial application. Factors such as pH and concentration of metal salt play key factors in exercising strict control over the morphology of biosynthesized nanoparticles (Gericke and Pinches 2006; Agnihotri et al. 2009; Pimprikar et al. 2009). Apart from the morphology of the biosynthesized nanoparticles, their purity as well as stability also play important role in determining their application for various purposes.

In the present research study, we have synthesized gold nanoparticles from the culture supernatant broth (SB) as well as the live cell filtrate (LCF) and live biomass solution (BS) of the filamentous fungus *Penicillium brevicompactum* KCCM 60390. The fungus is known to produce compactin which is an industrially useful metabolite and has been used for the synthesis of silver nanoparticles (Shaligram et al. 2009). The strain is important in food industries and used in fermentation for pectinase production (Pereira et al. 2002). We grew the fungus in potato dextrose broth (PDB). Later, it has also been able to synthesize gold nanoparticles. The time taken for synthesis in all the conditions was same except in case of BS where the time taken was longer as compared to PDB, SB, and LCF. Nanoparticles were found to be much dispersed and similar in shape and size following purification. However, the morphology of the nanoparticles synthesized from SB was better compared to LCF and PDB. Hence, further optimization was done to find the effect of pH and concentration of gold salt on SB for having strict control over the size and shape of the nanoparticles. Following optimization, gold nanoparticles were also used as a target material to check the percentage of cancer cell death at different incubation (24, 48, and 72 h) period. The viability of the cells was checked with well-known 3-(4, 5-dimethylthiazol-2-yl)-2, 5-diphenyltetrazolium bromide (MTT) method.

Materials and methods

Growth of microbial strain

The strain *P. brevicompactum* (KCCM 60390) was purchased from Korean Culture Centre of Microorganisms, Seoul, Republic of Korea. The above strain was initially grown on potato dextrose agar (PDA) plates at 30°C for 72 h. Isolated colonies obtained were restreaked into PDA slants and kept under refrigerated conditions for future use. For synthesis process, the strain was inoculated into PDB and agitated in a shaker incubator at 200 rpm for 72 h at 30°C. Following incubation, the culture SB was separated by filtering with Whatman filter paper no. 2. The biomass was harvested after 72 h of growth by sieving through a plastic sieve and washed thoroughly with sterile distilled (DI) water to remove any media component. In one set of experiment, the biomass obtained was inoculated in 30 ml of Milli-Q sterile deionized water and challenged with 20 ml of 1 mM gold salt. In another set of experiment, 5 g of this live biomass was further grown in 50 ml of Milli-Q sterile deionized water and agitated for 72 h at 200 rpm at 30°C. The resulting solution was filtered with Whatman filter paper no. 1. The supernatant obtained was LCF. Thirty-milliliter of LCF was challenged with 20 ml of 1 mM $HAuCl_4$ and incubated in shaker at 200 rpm under dark condition at 30°C. Dead biomass was prepared by resuspending the live biomass in sterile deionized water and autoclaving at 15 psi at 121°C for 15 min. Following this, the broth was filtered by using Whatman filter paper no. 1. The resulting dead biomass was washed with sterile deionized water to separate them from other media components. This was termed as dead cell filtrate (DCF).

Biosynthesis of gold nanoparticles

Twenty milliliters of 1 mM gold salt was challenged with 30 ml of LCF and DCF. The same procedure was also repeated with SB of the fungus. In another set of experiment, 20 ml of 1 mM gold salt was inoculated into 30 ml of sterile PDB. All the samples were inoculated in

shaker incubator at 200 rpm under dark condition at 30°C. Control was also run along with the experimental flasks containing only sterile PDB broth. Two milliliters of the samples were drawn at regular intervals for checking in UV–visible spectrophotometer (Shimadzu UV-1601) at a resolution of 1 nm. Following completion of synthesis, the samples were purified by centrifugation. Fifty milliliters of the as-synthesized gold nanoparticles dispersion is taken in the centrifuge tube. In our experiments, we adopted the DI water as the gradient solution. The aim of using the gradient solution was to improve the resolution of centrifugation through increasing the sedimentation distance of the particles. The DI water was firstly filled in the centrifuge tubes. Then, the as-synthesized gold nanoparticles dispersion was added on the top of the gradient solution. It was very important to choose the proper centrifugal run conditions. In our experiment, the sample of as-synthesized gold nanoparticles dispersion was centrifuged for half an hour at 10,000 rpm. After centrifugation, the supernatant solution of particles dispersion was collected. To improve the purity of the solution of nanoparticles, the process was repeated three times. The concentration of nanoparticles in the solution was expected to be decreased when centrifugation was repeated. The sediment possibly included large clusters of nanoparticles (in addition with some other impurities) which could be dispersed and centrifuged again so that more particles could be utilized effectively. The purified and unpurified samples were stored under refrigerated condition for characterization purpose.

Effect of reaction parameters

Effects of various reaction parameters which are expected to have potential impact on the quality of the nanoparticles (such as pH and concentrations of gold salt) were studied. In one set of experiment, the pH of the SB solution was varied (pH of 2, 4, 6, 8, and 10) and inoculated with 1 mM concentration of gold salt. In another set of experiment, the pH of the SB was kept constant (≈5.0) whereas varying amount of gold salt was inoculated into it (1, 2, 3, 4, and 5 mM). The samples synthesizing gold nanoparticles were purified in the same procedure as mentioned above and stored for characterization.

Characterization techniques

The morphology of the purified and unpurified gold nanoparticles was observed under Bio-TEM (HITACHI-JP/H7600). Bio-TEM images were also taken after storing the gold nanoparticles for 3 months under refrigerated condition for checking their stability. The average diameters and size distributions of Au nanoparticles were calculated by counting over 150 particles from the enlarged transmission electron microscopy (TEM) photography. The samples were prepared by putting a drop of solution on a copper carbon grid and setting the drop dry completely in a desiccator. Phase and crystal structure of the as-prepared gold nanoparticles were investigated by X-ray diffraction (XRD) technique (D/Max 2005, Rigaku). The gold nanoparticles as well as the control sample were given for Fourier transform infrared spectroscopy (FTIR; Shimadzu 8201PC, Japan) analysis for detecting changes in the surface functional groups.

Proliferation of cells

Mouse myoblast cancer cell C_2C_{12} were purchased from American Type Culture Collection (ATCC). The cells were thawed at 37°C in a water bath (Water bath DS-21L-Dasol, Scientific Co. Ltd, South Korea) for ~2–3 min and plated into 75-mm^2 flasks. After thawing, the cells were mixed with Dulbecco's modified Eagle's medium (DMEM) solution in centrifuge tube and centrifuged for 4 min at 15,000 rpm/min. The supernatant solution was discarded from the centrifuge tube, and cells were plated in 75 mm^2 with DMEM, 12% fetal bovine serum, and antibiotics (streptopenicillin and amphotericin B solution, Sigma) (10 ml/lit each) provided by ATCC. The cells were incubated for 24 h in a humidified environment with 5% CO_2 and 95% O_2.

After 24 h, the cells were humidified with 5% CO_2 and 95% air environment and washed with DPBS. The medium was replenished every other day. The cells were subcultured after they reached 50% confluence.

Cell viability by MTT method

The viability of the cells was checked by the well-known MTT assay. MTT powder (5 mg/ml) was prepared and stored as stock solution in dark place. The myoblast C_2C_{12} cancer cell lines were seeded into 96-well plates at 5.0×10^5 cell/well, and the plates were incubated overnight at 37°C in a humidification incubator with 5% CO_2. The stored stock of MTT solution was added to the control and treated (with gold nanoparticles–purified gold nanoparticles obtained from SB of the fungus) cell line samples and again incubated at 37°C for 3 h. After incubation, the samples were removed from incubator and mixed with solubilizing buffer. A purple color was visible at this stage and deepened over pipetting. The MTT solution was removed from the wells and mixed with solubilizing buffer. The control solution (without incorporation of gold nanoparticles/pure incubated cells) and treated samples (incubated cells incorporated with gold nanoparticles) were again incubated over night at 37°C to ensure that the formazan precipitate was dissolved. The measurement of MTT assay was analyzed with Elisa Reader (Bio Rad, M680) at 570 nm equipped with deuterium and xenon lamps.

Results

The colony morphology of the fungus when grown on PDA plates after 72 h of incubation at 30°C is shown in Fig. 1. Gold nanoparticles have been synthesized with PDB, SB, and LCF of *P. brevicompactum* to understand the chemistry of the nanoparticles formation. Visual observation confirmed the above fact as there was a gradual change in color of the medium after inoculation with 1 mM gold salt. This change was evident after 12 h of incubation. DCF of the fungus did not yield gold nanoparticles. Figure 2a–c shows the UV visible spectra for the synthesis of gold nanoparticles in LCF, PDB, and SB of *P. brevicompactum*, respectively. The live biomass of the fungus which was taken in 30 ml of deionized water and challenged with 20 ml of 1 mM gold salt changed purple in color. The purple biomass in the above solution was then filtered through Whatman filter paper no. 1 and then dried in a dry oven for few hours. Following filtration, the supernatant solution obtained (here referred as biomass supernatant solution (BSS)) was taken for UV–visible reading at different time intervals. However, no sharp peak was observed in this case. The UV reading was taken up to 24 h of incubation of the supernatant broth solution when kept at 30°C and 200 rpm in a shaker incubator under dark condition. The UV reading can be observed in Fig. 2e. The dry biomass obtained was further suspended in 10 ml of sterile deionized water and the UV reading of the BS was noted at regular intervals. It has been observed that the time of synthesis with the BS was prolonged as compared to the live cell filtrate and supernatant broth of the fungus. The total time taken was 48 h as increase in peak intensity was observed up to 48 h of incubation after which there was no further enhancement in peak showing complete synthesis of gold nanoparticles. The UV reading can be seen in Fig. 2f, g that shows the color of the dry biomass taken before synthesis and after challenged with 1 mM of gold salt.

Figure 3 shows the picture of the corresponding as-synthesized gold nanoparticles obtained from LCF, PDB, and SB of the fungus. Samples when withdrawn at regular time interval under UV–visible spectrophotometer showed an enhancement in peak at around 530~540 nm with increasing time of incubation. However, after 12 h, further enhancement in peak intensity was not been observed indicating completion of synthesis process.

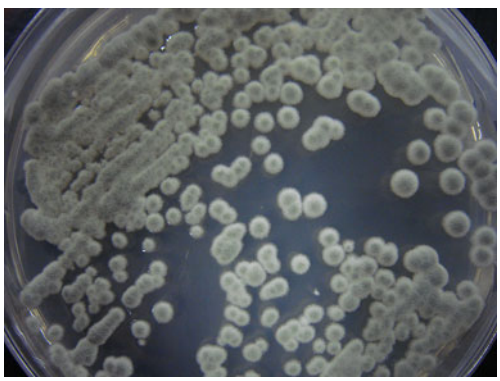

Fig. 1 Colony morphology of *P. brevicompactum* on PDA plate after 72 h of incubation

Fig. 2 UV–visible spectrum of time-dependent gold nanoparticles synthesis in the presence of **a** live cell filtrate of *P. brevicompactum* (LCF), **b** PDB broth (PDB), **c** supernatant broth of *P. brevicompactum* (SB), and **d** maximum intensity of the SP peak at different incubation time. **e** UV–visible spectra of biomass supernatant solution with respect to time at 30°C and 200 rpm, **f** UV–visible spectra of biomass solution with respect to time at 30°C and 200 rpm, and **g** visual observation in the color change of the dry biomass before and after nanoparticles synthesis

The morphology of the as-synthesized and purified nanoparticles is shown in Fig. 4. LCF has resulted in the synthesis of gold nanoparticles in the size range of 25 to 60 nm. Similarly, the size of the nanoparticles synthesized in PDB is about 20 to 80 nm. In this case, in addition to spherical gold nanoparticles, triangular- and hexagonal-shaped particles are also produced. SB has produced gold nanoparticles in narrow size range of 20 to 50 nm.

It is important to know the exact crystal structure of the gold particles formed, and this can be achieved by measuring the XRD spectrum of the samples. Phase of the as-prepared nanoparticles is investigated by X-ray diffraction technique, and corresponding XRD patterns are shown in Fig. 5. In each of the figures, gold nanoparticles have shown four distinct peaks at 2θ=38.37, 44.56, 64.74, and 77.29 corresponding to the (111), (200), (220), and (311) planes of the face entered cubic (FCC) structure of metallic gold. This result corresponds well to the standard XRD data (JCPDS no. 04-0784). The broadening of the X-ray peaks is primarily due to the small particle size of gold. The average particle diameter of the gold crystallites obtained by LCF, PDB, and SB are found to be 30, 45, and 60 nm, respectively, by using Scherrer's formula. Figure 6a–c shows the FTIR spectra of as-synthesized gold nanoparticles formed in LCF, PDB, and SB, respectively. All the spectra have shown clear peaks at 790, 1,670, 1,720, 2,970, and 3,410 cm^{-1}.

From the above results, it is assumed that the gold nanoparticles produced by SB are well dispersed and uniform in shape and size. Thus, we used particles synthesized by this process to investigate the effects of reaction parameters on the particle quality. Figure 7 shows the UV–visible spectrum of as-synthesized gold nanoparticles in SB after 12 h of incubation at different pH. It is observed that the peak due to the surface plasmon band centered around 525 to 550 nm at various pH. The intensity of the peak increased from pH 2 to 6 and then decreased. Figure 8 shows the picture of the corresponding gold nanoparticle dispersion at different pH. The color of the dispersion becomes darker with increase in the pH. Figure 9a–d shows the Bio-TEM images of the gold nanoparticles synthesized in SB at various pH. With increase

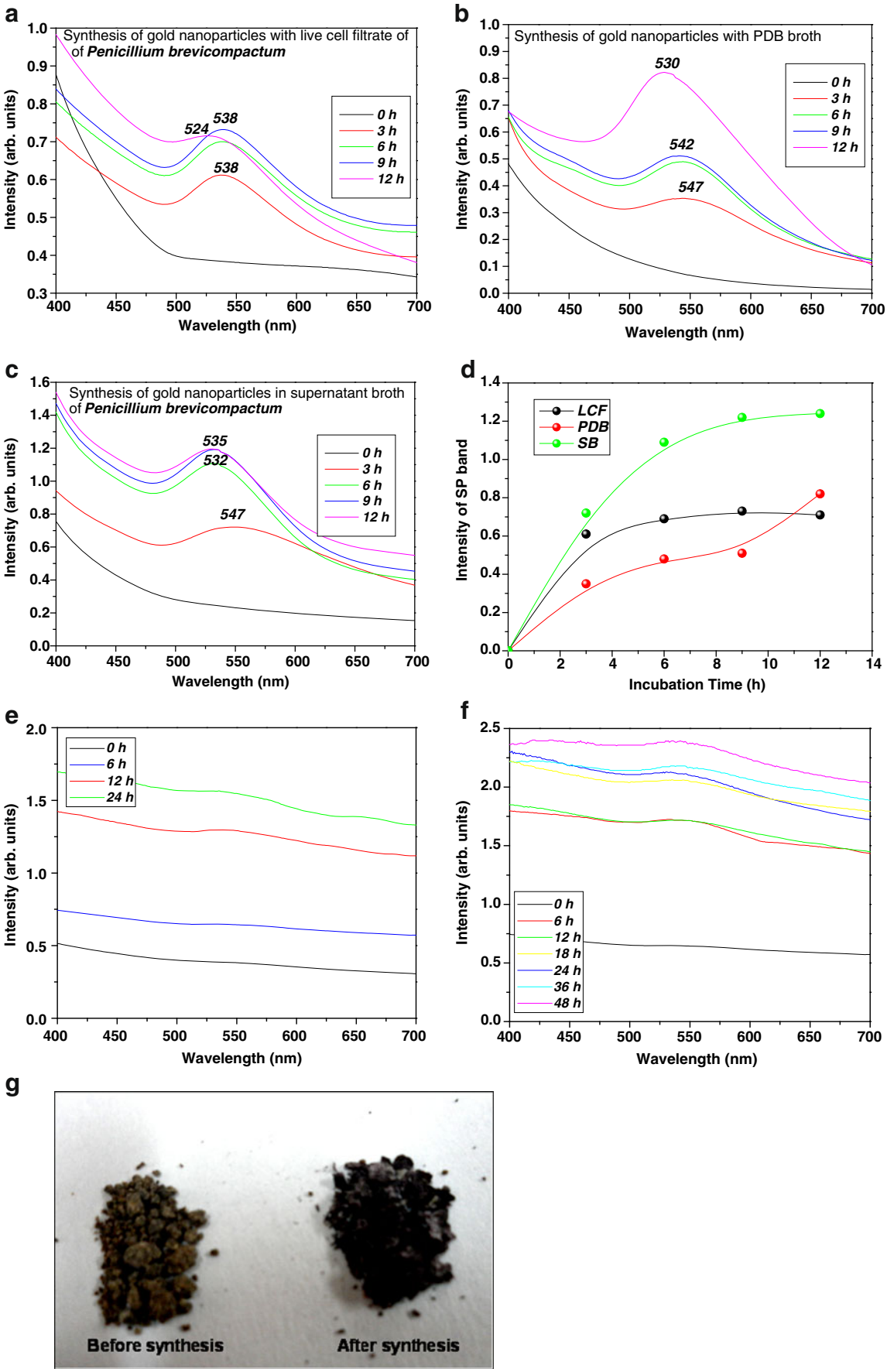
a
Synthesis of gold nanoparticles with live cell filtrate of of Penicillium brevicompactum
Intensity (arb. units)
Wavelength (nm)
524
538
538
0 h
3 h
6 h
9 h
12 h
b
Synthesis of gold nanoparticles with PDB broth
Intensity (arb. units)
Wavelength (nm)
530
542
547
0 h
3 h
6 h
9 h
12 h
c
Synthesis of gold nanoparticles in supernatant broth of Penicillium brevicompactum
Intensity (arb. units)
Wavelength (nm)
535
532
547
0 h
3 h
6 h
9 h
12 h
d
Intensity of SP band
Incubation Time (h)
LCF
PDB
SB
e
Intensity (arb. units)
Wavelength (nm)
0 h
6 h
12 h
24 h
f
Intensity (arb. units)
Wavelength (nm)
0 h
6 h
12 h
18 h
24 h
36 h
48 h
g
Before synthesis
After synthesis

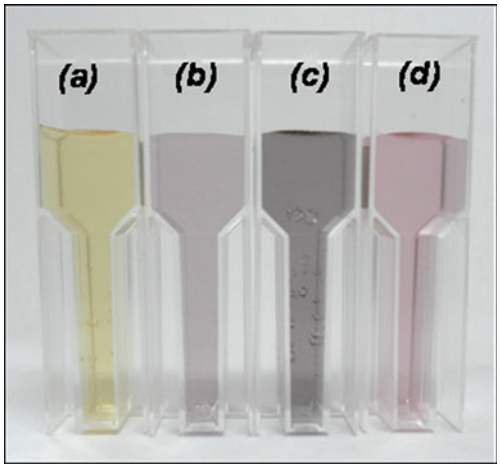

Fig. 3 Images of **a** control broth and as-synthesized gold nanoparticles in the presence of **b** live cell filtrate of *P. brevicompactum* (LCF), **c** PDB broth (PDB), and **d** supernatant broth of *P. brevicompactum* (SB) after 12 h of incubation with 1 mM gold salt

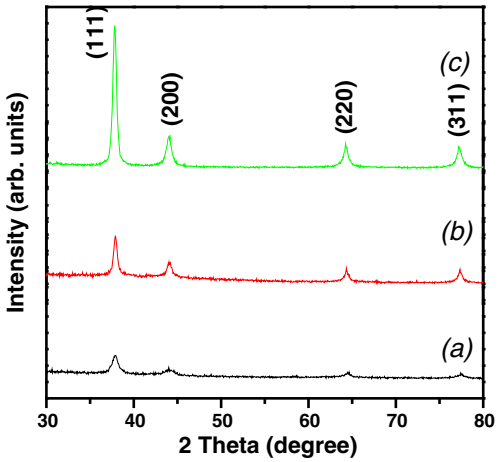

Fig. 5 XRD profile of purified gold nanoparticles obtained from **a** live cell filtrate of *P. brevicompactum*, **b** PDB broth, and **c** supernatant broth of *P. brevicompactum*

in the pH of the synthesis, medium remarkable change in the shape or size of the product is not noticed. However, pH 2 does not favor the synthesis because we could not find dispersed gold nanoparticles in TEM images. pH 6 and 8 have resulted in the production of quite well-dispersed nanoparticles with high particle density suggesting maximum yield. Beyond pH 8, slight increase in the size of the resultant nanoparticles is observed. The yield of the particle is also decreased beyond pH 8.

Figure 10 shows the UV–visible spectrum of gold nanoparticles synthesized by SB after 12 h incubation, at pH≈5 (natural pH of the system), with 1, 2, and 3 mM of the gold salt. Figure 11 shows the pictures of the corresponding gold nanoparticles dispersions. The color of the dispersion is pinkish red to light brown for 1 and 2 mM, respectively. But nanoparticle dispersion synthesized with 3 mM gold salt was less intense in color. Reaction mixture with 1 mM of the gold salt has resulted in the synthesis of near spherical particles in the size range of 10~50 nm with little aggregation (Fig. 12a). Similarly mixture with 2 mM of the gold salt has produced particles with broader size distribution (10~70 nm) (Fig. 12b). In this case, in addition to spherical particles, formation of triangular and hexagonal

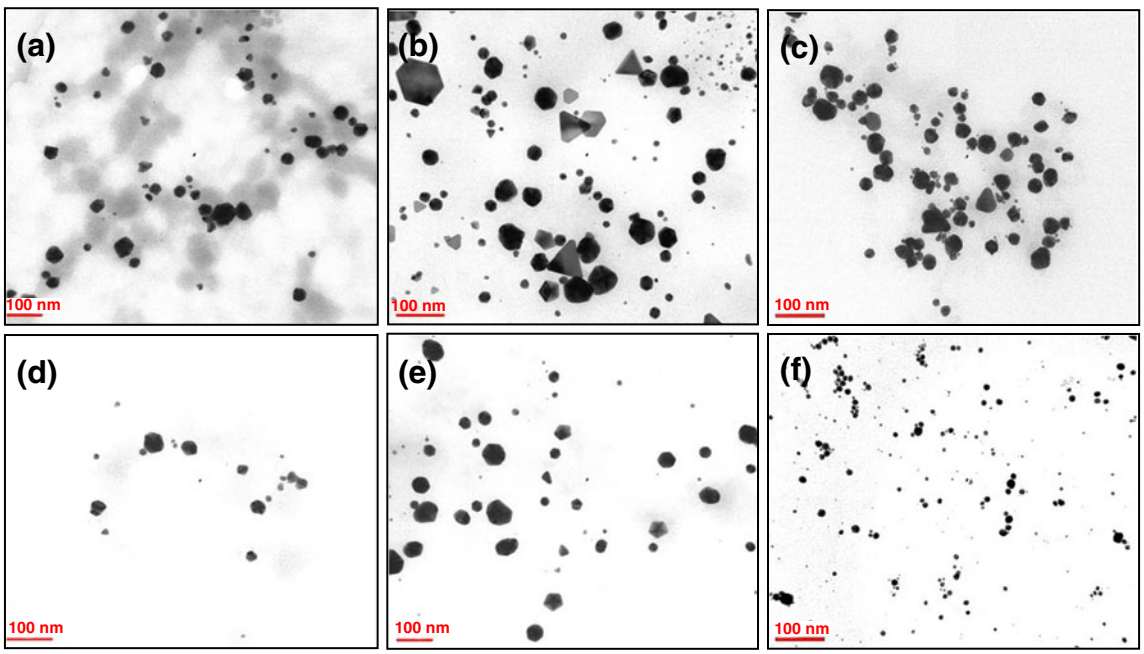

Fig. 4 Bio-TEM images of as-synthesized gold nanoparticles in presence of **a** live cell filtrate of *P. brevicompactum* (LCF), **b** PDB broth (PDB), and **c** supernatant broth of *P. brevicompactum* (SB) before purification. **d**–**f** The Bio-TEM images of the corresponding samples after purification. *Scale bar* is 100 nm

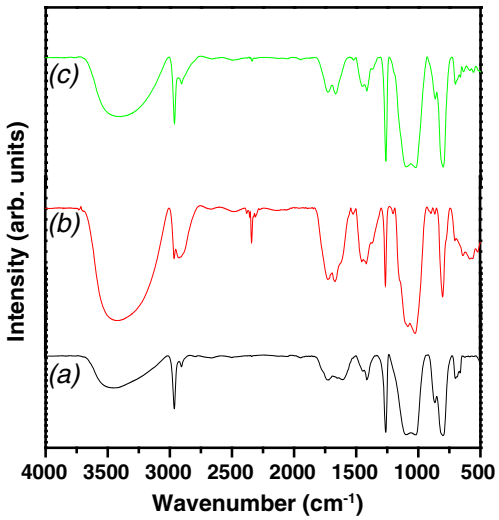

Fig. 6 FTIR spectra of purified gold nanoparticles obtained from **a** live cell filtrate of *P. brevicompactum*, **b** PDB broth, and **c** supernatant broth of *P. brevicompactum*

gold particles is also observed. Reaction mixture with 3 mM gold salt has resulted in the synthesis of larger particles (size range 50~120 nm) with spherical-, triangular-, and diamond-like morphologies (Fig. 12c).

To investigate the cause of low yield of gold nanoparticles in 3 mM gold salt concentration, we have checked the toxic effect of gold salt at different concentrations (1, 2, and 3 mM) on the growth of the fungus following synthesis. The SB of the fungus is obtained following incubation of the fungus into PDB broth at 30°C and 200 rpm shaking speed for 72 h. Thirty milliliters of the SB was challenged with 20 ml of 1, 2, and 3 mM gold salt each in separate conical flasks and incubated under dark in the

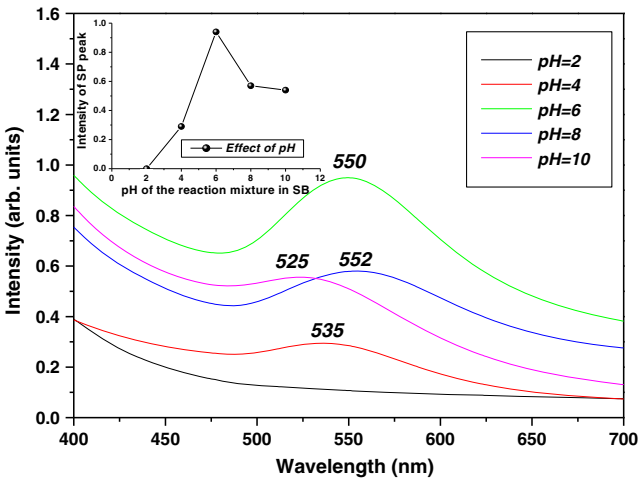

Fig. 7 UV–visible spectrum of gold nanoparticles synthesis reactions in presence of supernatant broth of *P. brevicompactum* at different pH with 1 mM gold salt after 12 h of incubation. *Inset* shows the pH vs maximum intensity of the SP peak after 12 h incubation

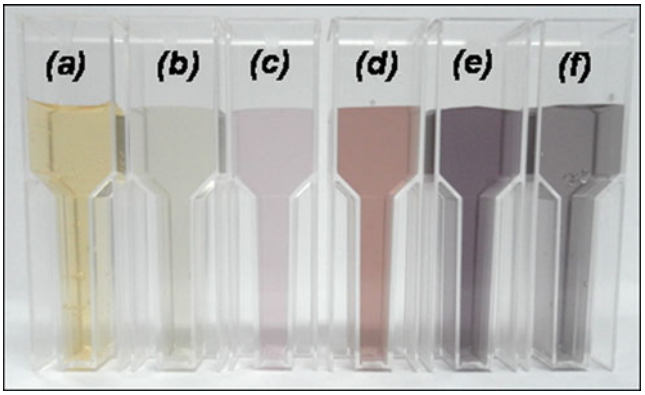

Fig. 8 Images of **a** control broth and as-synthesized gold nanoparticles in supernatant broth of *P. brevicompactum* at different pH (**b** pH 2, **c** pH 4, **d** pH 6, **e** pH 8, **f** pH 10) with 1 mM gold salt after 12 h of incubation

same experimental condition as mentioned above in the "Materials and methods" section. After 12 h of incubation, the synthesis was observed to be complete. After this, from each of the flasks, loopful of solution was taken and streaked onto PDA plates and kept at 30°C for 5 days. The results obtained on the PDA plates are given in Fig. 13 (a, b, and c for 1, 2, and 3 mM gold salt, respectively).

It is well-known fact that the practical application of metallic nanoparticles depends largely on their time-dependent stability. Thus, we investigated the stability of our gold nanoparticles for a period of 3 months. We have stored our dispersions in refrigerator and monitored the aggregation. Any precipitation is not observed even after 3 months of storage suggesting the gold nanoparticles have not aggregated. However, to get a direct evidence, we investigated the morphology and size by Bio-TEM, and corresponding images are shown in Fig. 14. The dispersity of the particles is quite well which rejects the possibility of any severe aggregation during storage period. Similarly, the size and shape of the nanoparticle are not changed noticeably suggesting the stability of the particles against any possible aggregation.

The MTT assay is a well-known calorimetric assay, which measures the cell proliferation rate. The activity of enzyme reduces the MTT (yellow color) into formazan salt, and it gives a purple color. This activity happens in the mitochondrial region and that way it measures the mitochondrial activity (Mosmann 1983). Apart from this, MTT is also used to determine the toxicity in the cells. The level of cytotoxicity or percentage (%) viability has been calculated in the following manner:

$$\%\ \text{viability} = [(\text{total cells} - \text{viable cells})/\text{total cells}] \times 100$$

or

$$\%\text{Viability} = \text{OD (optical densities) in sample well}/\text{OD in control well} \times 100$$

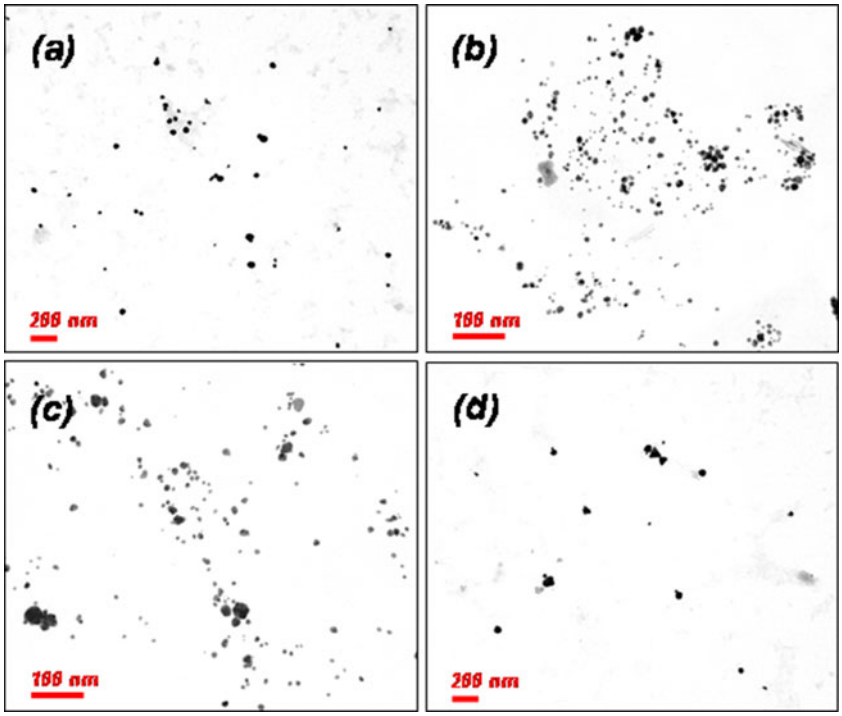

Fig. 9 Bio-TEM images of gold nanoparticles synthesized in supernatant broth of *P. brevicompactum* at pH=**a** 4, **b** 6, **c** 8, and **d** 10 after 12 h of incubation

MTT assay

Seeding of cells in 96 well plate (5.0×10^3 cells/well)

↓ 24 h

Treatment by synthesized compounds

↓ 24 h

Add MTT solution (10–20 μl to each well)

↓ 3 h

Discard media and add solublizing buffer solution (100 μl) to each well

↓ overnight stored at 37ºC in an incubator

Read immediately at 570 nm (Elisa reader) or store plate at –20ºC

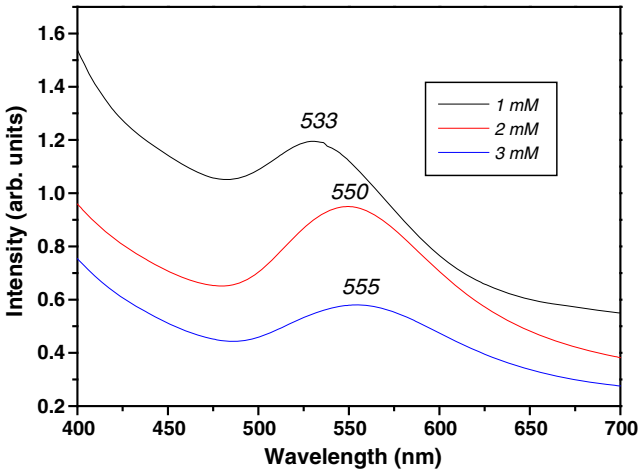

Fig. 10 UV–visible spectrum of gold nanoparticles synthesized in supernatant broth of *P. brevicompactum* at pH=5 with different concentration of gold salt after 12 h of incubation

The thiazol compound MTT has been widely used to measure the cell proliferation rate. The data obtained by MTT assay showed that different concentration of gold nanoparticles had inhibitory effects on the growth of C_2C_{12} cells in a dosage-dependent manner (Mosmann 1983). For survival studies, the cells were incubated at 37°C with and without incorporation of Au-NPs (200, 1,000, and 2,000 ng/ml) continuously. The cells were washed with PBS and to remove media DMEM. The cell survival was determined following addition of 200, 1,000, and 2,000 ng/ml of Au-NPs solution; 200, 1,000, and 2,000 ng/ml of Au-NPs at 24 h killed 21.4252%, 41.9226%, and 69.2110% of cells, respectively. The cell death after 48 h of incubation for the same concentration of NPs (200, 1,000, and 2,000 ng/ml) was 43.7720%, 73.7400%, and 81.7400%. As the incubation period of cells increased with the desired concentration of Au-NPs, the cell death increased correspondingly. After 72 h of incubation time, the cell death was 73.7200%, 89.8438%, and 92.6712% for 200, 1,000, and 2,000 ng/ml of Au-NPs solution, respectively (Fig. 15).

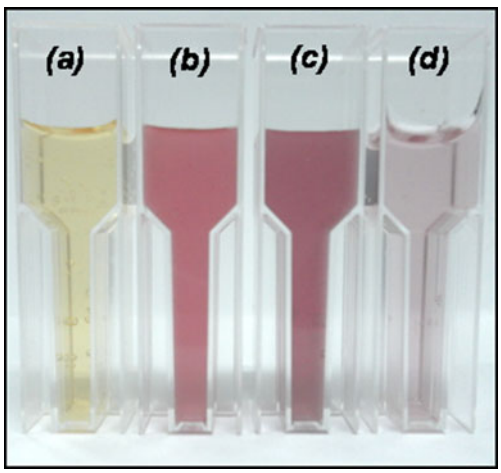

Fig. 11 Images of as-synthesized gold nanoparticles in supernatant broth of *P. brevicompactum* at pH=5 with **b** 1 mM, **c** 2 mM, and **d** 3 mM of gold salt following 12 h incubation

Discussion

The visual observation noticed in the change in color of the medium to intense pink upon 12 h of inoculation with the gold salt was the first confirmation showing the synthesis of gold nanoparticles in LCF, PDB, and SB as gold nanoparticles are known to exhibit vivid colors (Zinjarde and Pant 2002). Figure 2a–c has shown that gold surface plasmon (SP) peak has occurred at around 530~540 nm and steadily increased in intensity as a function of reaction time. The increase in intensity might be due to increasing number of nanoparticles formed as a result of reduction of gold ions present in the reaction solution. The intensity of the gold SP peak in the LCF has increased at 538 nm till 9 h suggesting the formation of nanosized particles. Beyond 9 h, the SP peak has blue-shifted to 524 nm with slight damping in the intensity. This suggests that the formation of gold nanoparticles is almost finished at 9 h by LCF. During synthesis, particles are expected to be capped with biomolecules which balances the electrostatic force around them and provides stability against aggregation. However, it is well-known that the SP peak of the metal nanoparticles is highly dependent on the shape, size, and surrounding chemical environment, and hence, any slight perturbation in these facts can lead to shift in the peak position (Ahmad et al. 2003a, b; Mulvaney 1996). It is expected that beyond 9 h, the gold nanoparticles have aggregated slightly due to Ostwald ripening phenomenon. Broadening of the SP peak also leads to the possibility of the increase in the amount of the biomolecules on the nanoparticles surface. However, it is expected that all the gold ions have not reduced to nanoparticles or simultaneous reduction and growth took place. Simultaneous reduction and growth may increase the Ostwald ripening and hence may lead to the formation of poorly dispersed particles with broad size distribution (Sugimoto 2003). The intensity of the peak after 12 h was only 0.75. This fact, along with TEM images, suggests that rate of the reaction is quite slow with minimum yield of the gold nanoparticles in LCF. In this case, synthesis is expected to be extracellular as suggested by Ahmad et al. (2003a, b), who have reported the synthesis of silver nanoparticles by fungus *Fusarium oxysporum*. It well-understood fact that nanoparticles formed on any kind of support can have smaller size (Narayanan and El-Sayed 2005). Thus, it is expected that the nanoparticles produced by LCF have smaller size (20 to 50 nm), where the metal nanoparticles are expected to be synthesized on the microbial cell wall. There are reports suggesting that

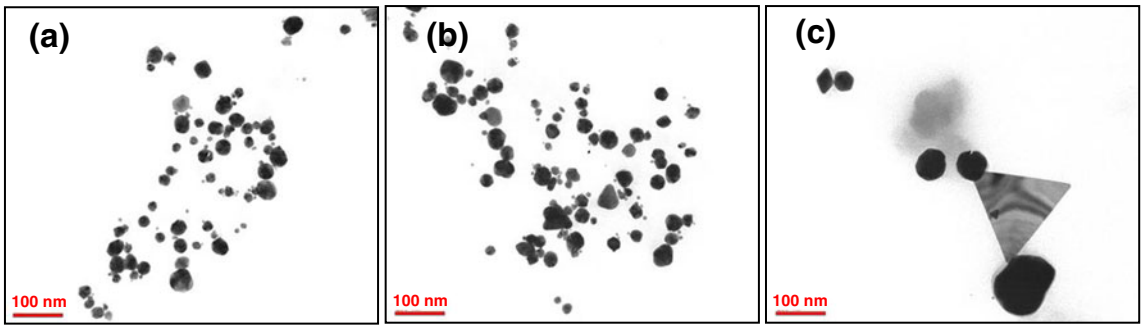

Fig. 12 Bio-TEM images of gold nanoparticles synthesized in supernatant broth of *P. brevicompactum* at pH=5 with different concentration of gold salt (**a** 1 mM, **b** 2 mM, and **c** 3 mM) after 12 h of incubation

trapping of gold ions on the surface of fungal cells can occur by electrostatic interaction with positively charged groups in enzymes that are present in cell wall of the mycelia (Mohanpuria et al. 2008). Gold nanoparticles produced by PDB broth have shown gradual and quite regular blue shift in the SP peak from 547 to 530 nm. It suggests that the formation of the gold nanoparticles and simultaneous encapsulation with biomolecules took place which has provided better stability against aggregation. Even after 12 h, the peak intensity has not damped, and further blue shift is restricted which may indicate the completion of the reaction. PDB contains dextrose and starch. Thus, formation of gold nanoparticles in PDB is similar to the reduction of gold ions by organic reducing agents such as urea or citric acid. To the best of our knowledge, any researcher has never reported the synthesis of metal nanoparticles in PDB. The above-mentioned biomolecules in PDB might not be present in case of LCF because of thorough washing to remove media components. Thus, the yield and stability of the metal nanoparticles is quite less in case of LCF than that of SB (which will contain the PDB along with the fungal cell). We have performed this experiment to know the actual chemistry of the nanoparticle formation. It is widely argued by different authors that the biochemicals secreted by microorganisms are particularly responsible for the synthesis of metallic nanoparticles (Mohanpuria et al. 2008; Duran et al. 2011). However, we demonstrated that it is not only the biochemicals (enzymes, proteins, cofactors, etc.) but also the organic reagents used for the microbial cultivations can act as potential reducing agents for the synthesis of metal nanoparticles. In the case of gold nanoparticles synthesized by PDB, the intensity of the SP peak after 12 h incubation is ~0.85. This observation in addition to the Bio-TEM images indicates the better yield of particles in PDB broth compared to LCF. In case of SB, SP peak blue-shifted from 547 to 535 nm with respect to the incubation time. From Fig. 2d, it is clear that the intensity of the SP peak is the highest for SB. These data in addition with the Bio-TEM images suggest maximum gold nanoparticle yield in this case. The synergetic effect of both PDB and microbial cell is expected to be the cause of the high yield of gold nanoparticles in SB. Bio-TEM images also suggests the formation of well-dispersed and uniform-sized particles with little aggregation. The rate of the reduction of the gold nanoparticles in both LCF and SB is expected to follow similar pattern, with high initial reaction rate between 3 and 6 h. Rate of the reaction reduced and finally becomes almost flat after 9 h. However, in case of PDB, slight increase in the rate of the reaction between 9 and 12 h is noticed. The authors remain unclear about the exact cause of this increase. Purification of nanoparticles by centrifugation has successfully removed aggregated and larger particles which is clearly evident in the Bio-TEM images. So, it can be expected that the purified samples can have better stability over a longer period of time which is further confirmed by Bio-TEM observations. From the results shown in Fig. 2a–g, it is also expected that although the

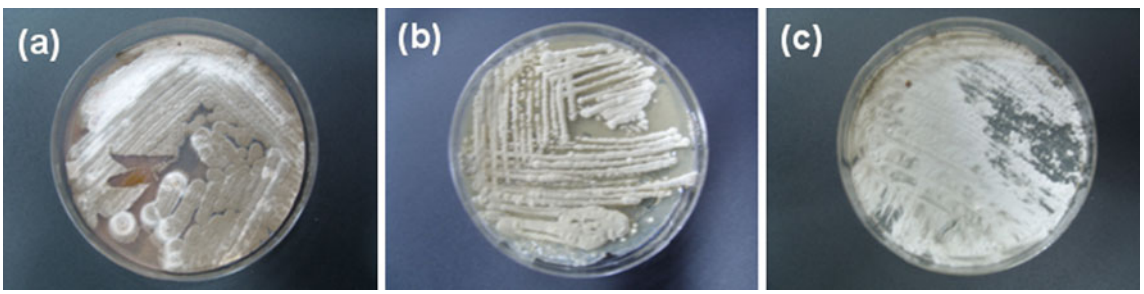

Fig. 13 Images of growth of the fungus on PDA plates following synthesis with 1, 2, and 3 mM gold salt

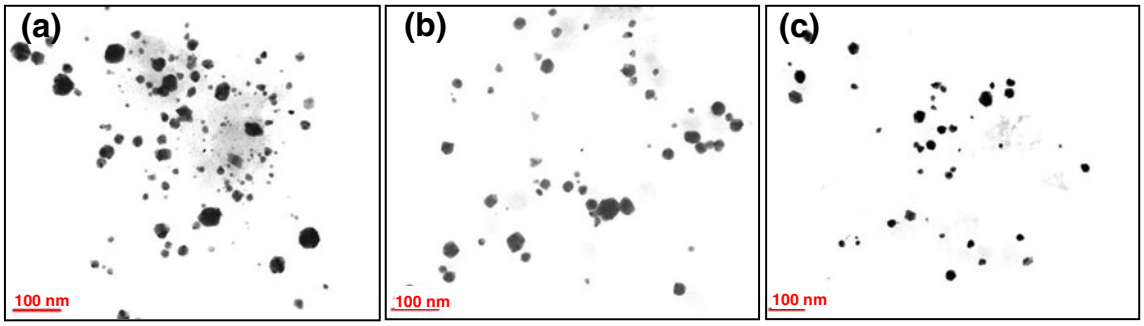

Fig. 14 Bio-TEM images of purified gold nanoparticles synthesized in **a** live cell filtrate of *P. brevicompactum* (LCF), **b** PDB broth (PDB), and **c** supernatant broth of *P. brevicompactum* (SB) after 3 months of preservation

reduction of gold ions is possible with biomass (BS) and perhaps also with BSS, the rate of the reaction and yield are significantly low. Comparing these results with the results obtained with SB and LCF, it can be suggested that the SB is the most active reducing agent for the synthesis of gold nanoparticles in the present case. The synergetic effect of both PDB and microbial cell is expected to be the cause of the fast and high yield of gold nanoparticles in SB.

The investigation of structure of the as-synthesized nanoparticles and nature of their surface chemical conditions is carried out by XRD and FTIR, respectively. XRD patterns have corresponded well to the standard FCC structure of the metallic gold. Absence of any other peaks suggests the formation of monophasic gold nanostructures. The broadening of the X-ray peaks is primarily due to the small particle size of gold. The slight shift in the peak position indicates the presence of strain in the crystal structure which is a characteristic of nanocrystallites. The slight difference in the particle size obtained from XRD analysis and direct visual observation in Bio-TEM suggests the polycrystalline nature of the as-synthesized nanoparticles (Cullity 1956). The FTIR spectrum of the gold nanoparticles synthesized by LCF, PDB, and SB has shown similar pattern. The complex nature of the peaks is expected due to presence of many biological molecules in the system. There is slight change in the intensity of the peaks in three different reaction systems. In particular, there is a broad peak in the range of 3,100 to 3,350 cm^{-1} which may corresponds to the stretching vibrations of OH or NH groups (Singh et al. 2010). In addition, there is strong peak around 2,970 cm^{-1} which may be the peak related to carboxylic and phenolic groups. Similarly absorption peaks due to amides may have shifted to 1,663 and 1,672 cm^{-1}. The peaks present near 800 cm^{-1} is attributed to R-CH groups. Similarly, a minor peak at 871 cm^{-1} may be due to Cl^- ion derived from $HAuCl_4$ (Pimprikar et al. 2009; Singh et al. 2010; Binupriya et al. 2010).

pH is considered an important factor when synthesizing bionanoparticles (Lim et al. 2011). As seen from Fig. 7, increase in the pH of the system has favored the formation of gold nanoparticles. At pH=2, formation of the gold nanoparticles is not observed. This may be due to the fact that high acidic condition can leach the gold nanoparticles surface easily (Habashi 1997). Formation of gold nanoparticles is evident by the existence of SP peak centered at 535 nm at pH=4. However, the intensity of the peak is too poor suggesting a poor yield of nanoparticles. Reaction at pH=6 has resulted in intense SP peak centered at 550 nm

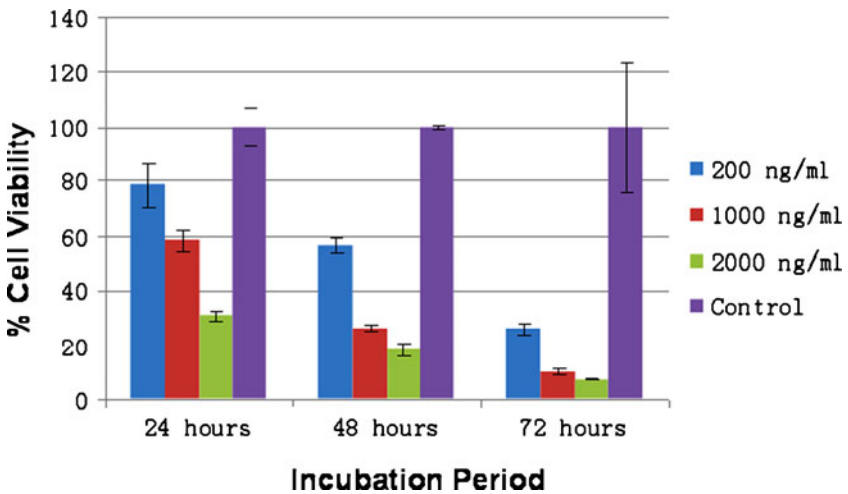

Fig. 15 MTT assay at different time intervals (24, 48, and 72 h)

suggesting the best synthesis condition. This is also supported from the picture of the dispersions (Fig. 8) and Bio-TEM images as shown in Fig. 9. Increase in the pH beyond 6 has resulted in the slight decrease in the yield and has significantly affected the gold nanoparticle quality at pH=10. This fact is strongly supported by the presence of aggregated nanoparticles at pH=8 and 10. The aggregation of nanoparticles has also resulted in the damping of the SP peak. Similar result is also reported by Liang and co-workers in the synthesis of gold nanoshells (Liang et al. 2011). Previously, we have observed optimum yield of gold nanoparticles at pH 4–6 with the yeast *Saccharomyces cerevisae* (Lim et al. 2011). Thus, optimum pH for the synthesis of gold nanoparticles is expected to be 5 to 8 in the present case. The effect of gold salt concentration is also investigated. Well-dispersed gold nanoparticles are formed at 1 mM of initial gold salt concentration in SB. With increase in the concentration to 2 mM, SP peak has shown a distinct red shift from 533 to 550 nm which suggests the formation of larger-sized nanoparticles which is also supported from the Bio-TEM images. It is well-known that the increase in the metal salt concentration will increase the nucleation process with the formation of larger and more number of nuclei which will subsequently lead to the formation of bigger particles with broader size distribution (Sugimoto 1987). Formation of larger particles along with aggregation may have resulted in the red shift and considerable damping of the SP peak at 2 and 3 mM salt concentration. At 3 mM initial salt concentration, very high nucleation rate in addition to prolonged growth process may have resulted in the formation of more diverse particle morphology such as triangular and hexagonal along with regular special shapes (Sugimoto 1989). In addition to this, the toxic effect of gold ions on the fungus is also another possible cause of low nanoparticle yield at higher salt concentration. It can be observed that for 1 mM gold salt, the growth of the fungus is faster and there has been complete mycelial formation with spores as can be evident from Fig. 13a. However in Fig. 13b, although mycelial formation can be seen, spores have not been completely formed and mat-like formation of the fungi is not observed as seen in the previous figure. In Fig. 13c, the fungus has grown very slowly, and only white colored mycelia are observed without any spore formation. Hence, it can be suggested that with increase in concentration of the gold salt, the biomolecules are slowly losing their activity as the growth rate is becoming slower. Gold salt is probably having toxic effect on the growth of the fungus which is why the reduction in UV peak intensity has been observed with increasing concentration of gold salt.

Stability of the purified nanoparticles is investigated, and their corresponding TEM images suggest their stability against aggregation even after 3 months (Fig. 14). The excellent stability is expected due to two important factors. First the aggregated and lager particles are removed during purification process. Thus, the resulting nanoparticles which are near homogenous in shape and size are expected to be more stable than the impure counter parts. Similarly, the presence of biological stabilizing agents may have contributed significantly to the increase in the stability of the dispersions by balancing the electrostatic force around the nanoparticles (Granqvist 1976).

Several groups have examined the cytotoxicity of gold nanoparticles (Connor et al. 2005; Chithrani et al. 2006; Patra et al. 2007). According to Pan et al., size of the gold nanoparticle plays a key role in inducing cytotoxicity in HeLa cells (Pan et al. 2007). Smaller size particles have better ability to induce cytotoxicity as compared to bigger ones. Hence, in our study, we have used the best synthesized gold nanoparticle (pH 6.00 with 1 mM gold salt obtained from SB of the fungus) after purification for studying their effect on cancer cell lines. It has been observed that the rate of cytotoxicity on the cell line has increased with the increase in incubation time with the gold nanoparticles. The enhanced effect is also noticed with increasing concentration of the nanoparticles as observed from Fig. 15. Although bulk gold has been reported to be safe (Murphy et al. 2008), nanoparticles of gold need to be examined for biocompatibility and environmental impact if they are to be manufactured on a large scale for in vivo usage (Colvin 2003; Shukla et al. 2005). Hence, further investigation and examination is required in using such particles as potential anticancer agents for therapeutic use.

The objective of our work is to synthesize gold nanoparticles through biological route by utilizing one of the industrially important strains *P. brevicompactum*. The mode of synthesis is extracellular as we got positive results with the LCF and SB of the fungus. Intracellular synthesis has also been observed with live biomass of the fungus, but rate of reaction in this case is observed to be very slow. Moreover, we also used PDB as a medium for synthesizing gold nanoparticles. The Bio-TEM images suggest that purified nanoparticles have better morphology as compared to unpurified ones. We compared the morphology of the purified nanoparticles obtained from all of the above routes, and since we got better results with SB of the fungus, we went for further optimization of the particles by altering the pH and concentration of the gold salt. pH 6 with 1 mM gold salt favored optimum synthesis of gold nanoparticles with well dispersity and similar morphology and a size range of 20 to 50 nm. The stability of bionanoparticles is also very important to be an alternative to chemically synthesized nanoparticles for various applications. From the Bio-TEM images observed in our results, there is not much aggregation or change in the size and shape of the particles even after 3 months of storage. Further, we studied the

effect of the nanoparticles synthesized from SB of the fungus at pH 6 with 1 mM gold salt on mouse cancer C_2C_{12} cell lines. The cytotoxicity occurred in a time-dependent manner. With more concentration of gold salt and increasing incubation time, the percentage of cell death increased. Although the nanoparticles have given effective cytotoxic activity, more extensive study is needed for suggesting them as potential anticancer agents. Even a thorough investigation is required for having an idea about the exact mechanism behind the formation of nanoparticles. We are trying to extend our results already obtained by undergoing more experiments to understand the mechanism for synthesis and also for targeting our nanoparticles in human cell lines for observing controlled cell death.

References

Agnihotri M, Joshi S, Kumar AR, Zinjarde S, Kulkarni S (2009) Biosynthesis of gold nanoparticles by the tropical marine yeast *Yarrowia lipolytica* NCIM 3589. Mater Lett 63:1231–1234

Ahmad A, Mukherjee P, Senapati S, Mandal D, Khan MI, Kumar R, Sastry M (2003a) Extracellular biosynthesis of silver nanoparticles using the fungus *Fusarium oxysporum*. Colloids Surf B 28:313–318

Ahmad A, Senapati S, Khan MI, Kumar R, Ramani R, Srinivas V, Sastry M (2003b) Intracellular synthesis of gold nanoparticles by a novel alkalotolerant actinomycete, *Rhodococcus* species. Nanotechnology 14(7):824–828

Binupriya AR, Sathishkumar M, Vijayaraghavan K, Yun SI (2010) Bioreduction of tri-valent aurum to nano-crystallite Au particles by active and inactive cells and cell free extract of *Aspergillus oryzae* var. *viridis*. J Hazard Mater 177:539–545

Chandran SP, Chaudhary M, Pasricha R, Ahmad A, Sastry M (2008) Synthesis of gold nanotriangles and silver nanoparticles using Aloe vera plant extract. Biotech Progress 22:577–583

Chithrani BD, Ghazani AA, Chan WCW (2006) Determining the size and shape dependance of gold nanoparticle uptake into mammalian cells. Nano Lett 6:662–668

Colvin V (2003) The potential environmental impact of engineered nanomaterials. Nature Biotechnol 21:1166–1170

Connor EE, Mwamuka J, Gole A, Murphy CJ, Wyatt MD (2005) Gold nanoparticles are taken up by human cells but do not cause acute cytotoxicity. Small 1:325–327

Cullity BD (1956) Elements of X-ray diffraction. Addison-Wesley, USA

Duran N, Marcato PD, Duran M, Yadav A, Gade A, Rai M (2011) Mechanistic aspects in the biogenic synthesis of extracellular metal nanoparticles by peptides, bacteria, fungi, and plants. Appl Microbiol Biotechnol 90:1609–1624

Ferrari M (2005) Cancer nanotechnology: opportunities and challenges. Nat Rev Cancer 5:161–171

Gardea-Torresdey JL, Parsons JG, Gomez E, Peralta-Videa J, Troiani HE, Santiago P, Yacaman MJ (2002) Formation and growth of Au nanoparticles inside live *Alfalfa* plants. Nano Lett 2:397–401

Gericke M, Pinches A (2006) Biological synthesis of metal nanoparticles. Hydrometal 83:132–140

Granqvist CG (1976) Ultrafine metal particles. J Appl Phys 47:2200–2220

Habashi F (1997) Handbook of extractive metallurgy. Wiley-VCH, Germany

Huang XH, Jain PK, El-Sayed IH, El-Sayed MA (2007) Size and concentration effect of gold nanoparticles on X-ray attenuation as measured on computed tomography. Nanomedicine 2:681–693

Kulkarni SK (2007) Nanotechnology: principles and practices. Capital, New Delhi

Liang Z, Liu Y, Ng SS, Li X, Lai L, Luo S, Liu S (2011) The effect of pH value on the formation of gold nanoshells. J Nanopart Res 13 (8):3301–3311

Lim H, Mishra A, Yun SI (2011) Effect of pH on the extra cellular synthesis of gold and silver nanoparticles by *Saccharomyces cerevisae*. J Nanosci Nanotech 11:518–522

Mandal D, Bolander ME, Mukhopadhyay D, Sarkar G, Mukherjee P (2006) The use of microorganisms for the formation of metal nanoparticles and their application. Appl Microbiol Biotechnol 69:485–492

Mishra A, Tripathy SK, Yun SI (2011) Bio-synthesis of gold and silver nanoparticles from *Candida guilliermondii* & their antimicrobial effect against pathogenic bacteria. J Nanosci Nanotech 11:243–248

Mohanpuria P, Rana NK, Yadav SK (2008) Biosynthesis of nanoparticles: technological concepts and future applications. J Nanopart Res 10:507–517

Mosmann T (1983) Rapid colorimetric assay for cellular growth and survival: application to proliferation and cytotoxicity assays. J Immunology Methods 65:55–63

Mukherjee P, Ahmad D, Mandal A, Senapati S, Sainkar SR, Khan MI, Parishcha R, Ajay Kumar PV, Alam M, Kumar R, Sastry M (2002) Extracellular synthesis of gold nano particles by the fungus *Fusarium oxysporum*. Chem Bio Chem 3:461–463

Mulvaney P (1996) Surface plasmon spectroscopy of nanosized metal particles. Langmuir 12(3):788–800

Murphy CJ, Gole AM, Stone JW, Sisco PN, Alkilany AM, Goldsmith EC, Baxter SC (2008) Gold nanoparticles in biology: beyond toxicity to cellular imaging. Acc Chem Res 41:1721–1730

Narayanan R, El-Sayed MA (2005) Catalysis with transition metal nanoparticles in colloidal solution. J Phys Chem B 109 (26):12663–12676

Pan Y, Neuss S, Leifert A, Fischler M, Wen F, Simon U, Schmid G, Brandau W, Jahnen-Dechent W (2007) Size dependant cytotoxicity of gold nanoparticles. Small 3:1941–1949

Park TJ, Lee SY, Heo NS, Seo TS (2010) In-vivo synthesis of diverse metal nanoparticles by recombinant *E. coli*. Angew Chem Int Ed 49(39):7019–7024

Patra HK, Banerjee S, Chaudhuri U, Lahiri P, Dasgupta AK (2007) Cell selective response to gold nanoparticles. Nanomedicine 3:111–119

Peer D, Karp JM, Hong S, Farokhzad OC, Margalit R, Langer R (2007) Entrapment of hydrophobic drugs in nanoparticle monolayers with efficient release into cancer cells. Nat Nanotechnol 2:751–760

Pereira JF, Queiroz MV, Gomes EA, Muro-Abad JI, Araújo EF (2002) Molecular characterization and evaluation of pectinase and cellulase production of *Penicillium* spp. Biotechnol Lett 24:831–838

Pimprikar PS, Joshi SS, Kumar AR, Zinjarde SS, Kulkarni SK (2009) Influence of biomass and gold salt concentration on nanoparticle synthesis by the tropical marine yeast *Yarrowia lipolytica* NCIM 3589. Colloids Surf B Biointerf 74:309–316

Shaligram NS, Bule M, Bhambure R, Singhal RS, Singh SK, Szakacs G, Pandey A (2009) Biosynthesis of silver nanoparticles using aqueous extract from the compactin producing fungal strain. Process Biochem 44:939–943

Shankar SS, Ahmad A, Pasricha R, Sastry M (2003) Bioreduction of chloroaurate ions by geranium leaves and its endophytic fungus yields gold nanoparticles of different shapes. J Mater Chem 13:1822–1826

Shukla R, Bansal V, Chaudhary M, Basu A, Bhonde R, Sastry M (2005) Biocompatibility of gold nanoparticles and their endocy-

totic fate inside the cellular compartment: a microscopic overview. Langmuir 21:10644–10654
Singh AK, Talat M, Singh DP, Srivastava ON (2010) Biosynthesis of gold and silver nanoparticles by natural precursor clove and their functionalization with amine group. J Nanopart Res 12:1667–1675
Sugimoto T (1987) Preparation of monodispersed colloidal particles. Adv Colloid Interface Sci 28:65–108
Sugimoto T (1989) Preparation and characterization of monodispersed colloidal particles. Mater Res Soc Bull 14:23–28
Sugimoto T (2003) Formation of monodispersed nano- and microparticles controlled in size, shape, and internal structure. Chem Eng Technol 26:313–321
Torchilin VP (2006) Multifunctional nanocarriers. Adv Drug Delivery Rev 58:1532–1555
William D (2004) Applications of nanoparticles in biology and medicine. J Nanobiotechnol 2:1–6
Zinjarde SS, Pant A (2002) Hydrocarbon degraders from tropical marine environments. Marine Poll Bull 44:118–121